Experimental Study of Spark-Ignition Combustion using the Anode Off-Gas from a Solid Oxide Fuel Cell

Author, co-author (Do NOT enter this information. It will be pulled from participant tab in MyTechZone)

Affiliation (Do NOT enter this information. It will be pulled from participant tab in MyTechZone)

Abstract

Hybridizing Solid Oxide Fuel Cells (SOFCs) with internal combustion engines is an attractive solution for power generation at high electrical conversion efficiency while emitting significantly reduced emissions than conventional fossil fueled plants. The gas that exits the anode of an SOFC operating on natural gas is a mixture of H_2, CO, CO_2, and H_2O vapor, which are the products of the fuel reforming and the electrochemical process in the stack. In this study, experiments were conducted on a single-cylinder, spark-ignited Cooperative Fuel Research Engine using the anode off-gas as the fuel, at compression ratio of 11:1 and 13:1, engine speed of 1200 rev/min and intake pressure of 75 kPa, to investigate the combustion characteristics and emissions formation. A comparison was drawn with combustion with Compressed Natural Gas (CNG) at the same engine operating conditions. The experimental results revealed that the anode off-gas can be used as a potential alternative fuel for spark-ignition combustion, and an engine can be used to provide additional power to a hybrid SOFC-engine system. Combustion with the anode off-gas resulted in similar net indicated efficiency with CNG at CR of 13:1, but with negligible NO_x emissions and zero total hydrocarbon emissions. However, combustion with the anode off-gas resulted in lower volumetric efficiency and lower load than CNG as a result of high levels of dilution in the off-gas, which greatly reduces the lower heating value of the fuel. This study demonstrated the feasibility of using the SOFC anode-off gas as a potential fuel for spark-ignition engines with good fuel conversion efficiency and minimal NO_x and THC emissions.

Introduction

The growing concerns of environmental sustainability caused by continuous increases in worldwide energy demands, have shifted attention to novel and innovative energy conversion technologies such as solar power, wind power, and fuel cells, as they are seen as environmentally friendly solutions for power generation. Particularly, Solid Oxide Fuel Cells (SOFC) have high electrical conversion efficiency since the electricity is directly generated by fuel oxidization in the cathode instead of through combustion, and with significant reduction in pollutant formation compared to other power generation technologies that are currently used [1-4]. Efforts have been made to understand the ways of improving the SOFC electrical conversion efficiency, such as system level optimization of fuel cell stack configurations, cell stack performance improvement, as well as hybridizing SOFCs with other energy conversion devices [5, 6].

Some studies have investigated hybridizing SOFCs with Gas Turbines (GTs) to improve electrical conversion efficiency with system capital cost reduction [7-9]. In a SOFC-GT hybrid system, the high temperature anode off-gas is burned in a combustor and then expanded in a turbine to generate additional power [10-12]. Although the SOFC-GT hybrid systems provide efficiency advantages, they have mostly been demonstrated for large scale power generation applications due to limitations in size, cost, and operating conditions of the gas turbines.

On the other hand, combining SOFCs with internal combustion engines can be more suitable for transportation applications since engines are produced in a large range of sizes and power outputs. Previous studies have shown that IC engines can have a distinct advantage when compared to gas turbines in terms of efficiency and cost at small scale [13, 14]. In a SOFC-ICE hybrid system, the highly diluted anode off-gas can be used as the fuel for the engine to generate additional power for the system. Kim et al. [15] experimentally investigated the use of SOFC anode off-gas as a fuel using spark-assisted compression ignition with indicated efficiency of 61.6% for the hybrid system and ultra low NO_x emissions. Fyffe et al. [16] presented a theoretical study on mixed combustion-electrochemical energy conversion using fuel cells coupled to internal combustion engines and concluded that this concept holds promise for reaching 70% electrical conversion efficiency for medium-scale systems. Choi et al. [17] experimentally investigated a solid oxide fuel cell – homogeneous charge compression ignition (SOFC-HCCI) system to investigate the potential of using the anode off-gas in a low temperature combustion mode. They reported a gross indicated efficiency of 30% achieved with nearly zero NO_x and THC emissions. However, the dilute nature of the anode off-gas required very high compression ratio and/or intake air preheating in order to achieve stable autoignition in HCCI mode. The composition of the anode off-gas makes it conducive to SI combustion, either stoichiometric or lean, that can offer similar benefits to low temperature combustion without the need for complicated control.

Spark-ignition engines have advantages in direct control of the start of combustion and can use an effective three-way catalyst for reduction of pollutant emissions compare to low temperature combustion modes. The anode off gas contains H_2, CO, CO_2, and H_2O, which is syngas (H_2 + CO) dilute with CO_2 and water vapor. Previous experimental studies from the authors revealed that syngas is a viable alternative fuel for SI combustion and can offer higher efficiency and lower emissions compared to conventional hydrocarbon fuels [18]. The laminar flame speed of hydrogen is the highest among all gaseous fuels, and its requirement of ignition energy is also the lowest [19], thus enabling lean or dilute stoichiometric SI combustion.

Gaseous fuels such as Compressed Natural Gas (CNG) and syngas have been used as alternative fuels for spark-ignition combustion due to their favorable physical and chemical properties. CNG is an attractive alternative fuel that is logistically available and economical compared to conventional gasoline. It consists primarily of methane (CH_4) at concentrations of 85-97% vol. [20], with other constituents such as ethane, propane, butane, and diluents such as nitrogen and carbon dioxide. Its high hydrogen to carbon (H/C) ratio results in lower CO_2 emissions than gasoline [21]. The research octane number (RON) for CNG is high (~130), which offers excellent resistance to knock and enables engine operation at higher compression ratios for improved efficiency.

Syngas is also a gaseous fuel that consists of H_2 and CO in various blends, depending on its source and production pathway. The energy density of syngas is lower than conventional hydrocarbon fuels due to the considerably low density of H_2 and CO [22]. Consequently, combustion with syngas is expected to produce less work when compared to CNG at the same engine operating conditions. In addition, the engine volumetric efficiency is reduced when using syngas since the LHV is reduced greatly which necessitates higher fuel flow rates than CNG. The RON of hydrogen is also high (RON~120), which enables operation at higher compression ratios. The absence of hydrocarbon compounds in syngas also results in negligible THC emissions [23]. Since the anode off-gas contains syngas with high levels of diluents (CO_2 and H_2O), it is expected that SI combustion with off-gas will result in lower heat release than CNG fuel, but also lower emissions.

Limited experimental and computational studies have been performed to investigate and quantify the feasibility, performance, combustion characteristics, and exhaust emissions using the SOFC anode off-gas as a fuel in spark-ignition combustion. The objective of this experimental study is to investigate how the highly diluted anode off-gas can be used as a potential alternative fuel for SI engines, with the goal of using an engine in a hybrid SOFC-ICE system. Also, the anode off-gas is compared against CNG at the same operating conditions. This comparison has been conducted at compression ratios of 11:1 and 13:1. The following sections describe the experimental setup and methodology, and the experimental results and analysis.

Experimental Set-Up and Methodology

Experimental studies were performed in a single-cylinder, four stroke, spark-ignited Cooperative Fuel Research (CFR) engine mounted on an active DC dynamometer. The engine cylinder features an overhead two valve system and a side mounted spark plug. The CFR engine has variable compression ratio, ranging from 6:1 to 18:1. Engine relevant specifications are summarized in Table 3, and a schematic diagram of the CFR engine setup is shown in Figure 1. The intake air flow rate was measured and regulated using an Alicat MCRW-500SLPM-D/5M mass flow controller located upstream of the intake plenum. Gaseous fuel flow was measured with an Alicat MCR-200SLPM-D/5M mass flow controller and fumigated into the intake plenum where it was mixed with incoming intake air to form a homogeneous air-fuel charge. The cylinder pressure was measured with a Kistler 7061B piezoelectric pressure transducer mounted in the cylinder head. The crankshaft position was measured using a BEI XH25D-SS-1024 crank angle encoder featuring a 0.2 crank angle degrees (CAD) resolution. The spark plug ignition timing and port-fuel injector timings were determined using a Performance Electronics PE3 engine control unit set to manual entry. A Horiba MEXA-7100DEGR exhaust gas analyzer was used for measuring CO, CO_2, O_2, THC, and NO_x emissions. The data acquisition system was built based on a National Instruments cDAQ chassis for measurements of low speed and high speed data.

All of the experimental studies were conducted on the CFR engine at constant engine speed of 1200 rev/min with intake pressure of 75 kPa and ambient temperature of 300K. The compression ratio was set at 11:1 and 13:1. During the experimentation, spark timing was swept to find the Maximum Brake Torque (MBT) for each operating point. For CNG, the equivalence ratio was swept from stoichiometry ($\phi = 1.0$) by step of 0.05 until the lean misfire limit was approached (defined as COV IMEP $\geq$ 5%). As for the anode off-gas, the equivalence ratio was swept from stoichiometry down to $\phi = 0.60$ in 0.05 decrements.

A detailed schematic of the proposed SOFC-ICE hybrid system is presented in Figure 2. This hybrid plant is composed of two major energy conversion devices which are the high-temperature pressurized SOFC stack and the spark ignition internal combustion engine. The measured anode off-gas composition exiting the stack is 17.1% H_2, 7.9% CO, 25.4% CO_2, and 49.6% H_2O, as summarized in Table 1. These measurements were performed on a nominal operating point of a 5 kW SOFC stack with 65% gross electrical efficiency, at 68% fuel utilization and 51.1% anode recycle. This composition contains nearly 25% syngas (H_2 + CO) by volume and is highly diluted with water vapor and CO_2 resulting from the electrochemical process. Given that high levels of dilution, the fuel energy content for the anode off-gas is significantly lower than any conventional hydrocarbon fuels, which will affect the combustion process. Consequently, it is deemed necessary to remove the water vapor content out of the anode off-gas to increase the energy content and flame speed. Therefore, an anhydrous anode off-gas featuring a composition of 33.9% H_2, 15.6% CO, and 50.5% CO_2 is proposed and used for the experimental studies, summarized in Table 1 as well. The relevant fuel properties for the anode off-gas and CNG are listed in Table 2 below.

Table 1. Anode off-gas composition for a 5 kW SOFC stack with 65% electrical efficiency, 68% fuel utilization, and 51.1% anode recycle.

Composition	H_2	CO	CO_2	H_2O
Wet (Actual)	17.1%	7.9%	25.4%	49.6%
Dry	33.9%	15.6%	50.5%	0%

Table 2. Relevant fuel properties for the anode off-gas and CNG.

Fuels	Anode Off-Gas (dry)	CNG
Formula	$C_{0.66}H_{0.68}O_{1.16}$	$C_{1.01}H_{3.97}O_{0.01}N_{0.03}$
MW [g/mole]	27.16	16.67
H/C Ratio	1.03	3.93
LHV [MJ/kg]	4.69	47.62
C_p [KJ/Kg-K]	1.21	2.34
Stoich AFR	1.26	16.29

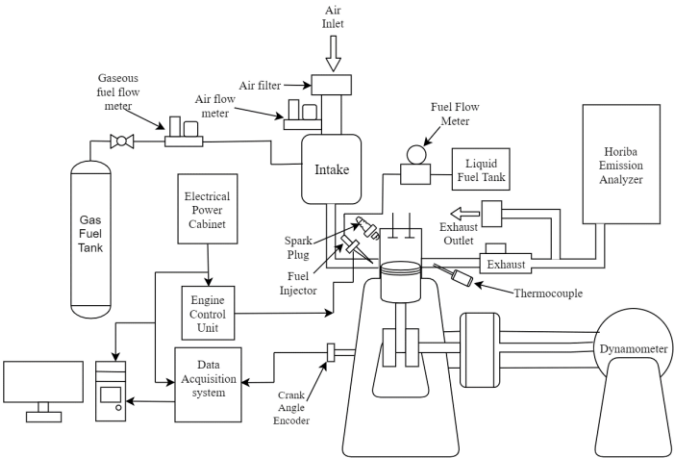

Figure 1. Schematic diagram of the experimental set-up.

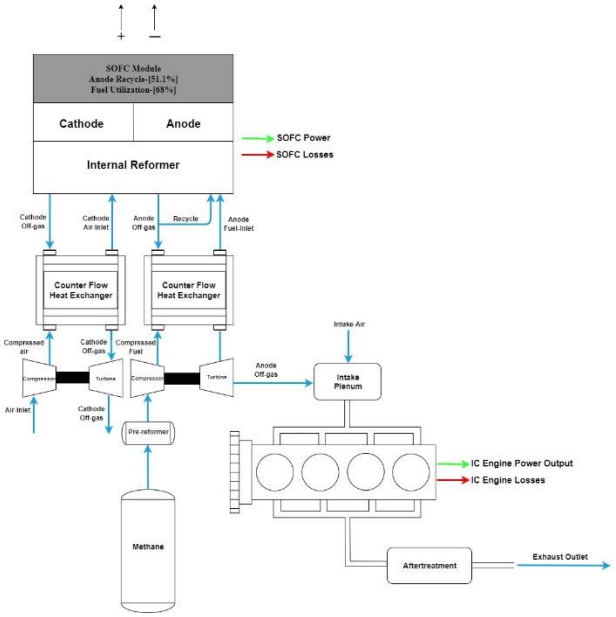

Figure 2. Schematic diagram for the proposed SOFC-ICE hybrid system

Table 3. CFR engine detailed specifications.

Specification	Quantity
Number of Cylinders	1
Number of Valves	2
Stroke	114.3 mm
Bore	82.6 mm
Displaced Volume (cm^3)	611.7 cm^3
Intake Valve Opening (IVO)	-350° aTDC
Intake Valve Closing (IVC)	-146° aTDC
Exhaust Valve Opening (EVO)	140° aTDC
Exhaust Valve Closing (EVC)	-345° aTDC
Compression Ratio	6:1 – 18:1
Fueling Method (liquid fuel)	Port fuel injection
Fueling Method (gaseous fuel)	Fumigated
Engine Revolution Speed (RPM)	1200

Results and Discussion

The engine volumetric efficiency, η_V, is a parameter used to quantify the effectiveness of an engine's intake process [24], and it is calculated based on the mass of air trapped in the cylinder, m_a; the intake air density, $\rho_{a,i}$; and the engine displaced volume, V_d:

$$\eta_V = \frac{m_a}{\rho_{a,i} V_d} \quad (1)$$

The volumetric efficiency of the CFR engine operating with anode off-gas and CNG is shown in Figure 3 as a function of fuel-air equivalence ratio, ϕ, for CR of 11:1 and 13:1. Overall, the volumetric efficiency increased for both fuels as the ϕ was decreased from stoichiometry, due to the increasing amount of intake air flowing into the cylinder.

Additionally, as the compression ratio was increased from 11:1 to 13:1, the volumetric efficiency increased because of decreasing residual gas fraction. The volumetric efficiency for anode off-gas is significantly lower compared to CNG. This difference results primarily from the lower stoichiometric air-fuel ratio of 1.25:1 for anode off-gas, versus 16.3:1 for CNG, which necessitates a high amount of gaseous fuel entering the cylinder thus displacing fresh air. In addition, the anode off-gas contains 50.5% of CO_2 by volume, which is a diluent and reduces the energy density of the mixture, thus increasing the required fuel flow and exacerbating the air displacing effect.

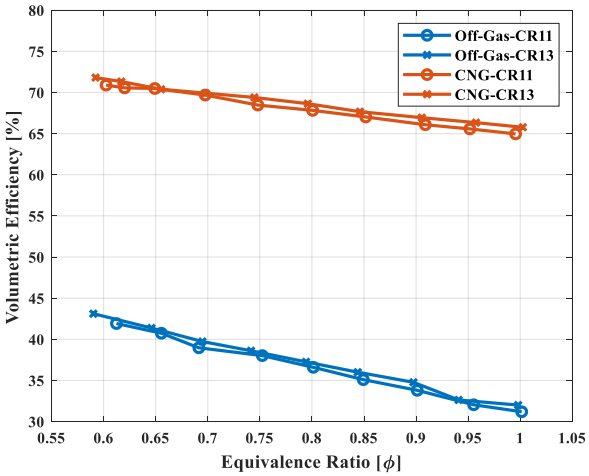

Figure 3. Volumetric efficiency as a function of φ for the anode off-gas and CNG.

The net indicated mean effective pressure, $IMEP_{net}$, is a standard analytical parameter used to quantify the capacity of an engine to produce work, independent of displacement volume, calculated based on in-cylinder pressure data. Figure 4 displays the $IMEP_{net}$ for both fuels with respect to equivalence ratio. The $IMEP_{net}$ is shown to proportionally decrease with equivalence ratio for both compression ratios studied. This relationship is expected given that leaner air-fuel mixtures contain less energy. Additionally, enleanment of the air-fuel mixture results in decreased flame speeds which in turn causes reduction in heat release rates and explain the observed trend between $IMEP_{net}$ and ϕ. Increasing the CR from 11:1 to 13:1 did not yield a significant increase in engine load for either fuel. The higher compression ratio experimental data set indicated that operating conditions were knock-limited, so spark timing had to be retarded from the optimal, maximum brake torque, timing. Combustion with the anode off-gas resulted in significantly lower engine load at a given compression ratio and equivalence ratio when compared to CNG, as a result of the lower volumetric efficiency, lower stoichiometric air-fuel ratio, and reduced lower heating value (LHV), which resulted in higher fuel flow rate required.

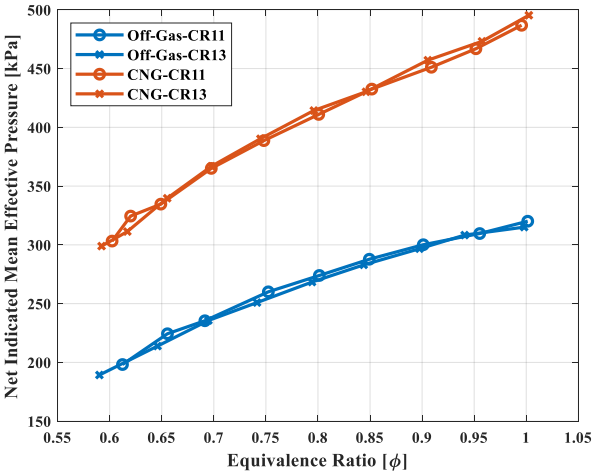

Figure 4. Engine $IMEP_{net}$ as a function of φ for the anode off-gas and CNG.

Figure 5 compares the apparent heat release rate for the anode off-gas and CNG at compression ratio of 11:1 and 13:1 at stoichiometry. Combustion with the anode off-gas resulted in lower heat release rate at given compression ratios compared to CNG, due to its slower flame propagation caused by the diluents in the fuel mixture. Increasing the compression ratio resulted in a decrease in heat release rate and elongated burn duration due to the fact that spark timing was retarded to avoid end-gas knock.

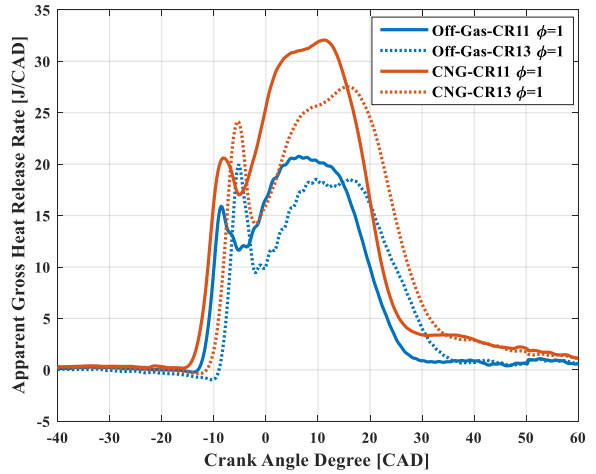

Figure 5. Apparent heat release rates for the anode off-gas and CNG.

The peak cylinder temperature with respect to ϕ, for the anode off-gas and CNG combustion, at CR of 11:1 and 13:1 is shown in Figure 6. The ideal gas law is used to calculate the mass-averaged cylinder bulk temperature as a function of crank angle, based on the measured cylinder pressure, $P_{cyl}(i)$, the instantaneous cylinder volume, $V(i)$, the total trapped cylinder mass, $mass_{cyl}$, and the gas constant, R.

$$T_{Bulk}(i) = \frac{P_{cyl}(i) * V(i)}{mass_{cyl} * R} \qquad (2)$$

As expected, the peak cylinder temperature decreases proportionally with decreasing ϕ due to the reduction in heat release. Increasing the compression ratio requires retarding the spark timing to avoid end-gas

knock, which overall decreases the peak cylinder temperature. Combustion with the anode off-gas has lower peak cylinder temperature compared to CNG because of (i) the lower volumetric efficiency, which reduces the overall mass of the air-fuel mixture content in the cylinder, (ii) the significantly lower LHV of the anode off-gas, and (iii) the diluents in the off-gas which act as a heat sink during combustion, in a similar manner to exhaust gas recirculation.

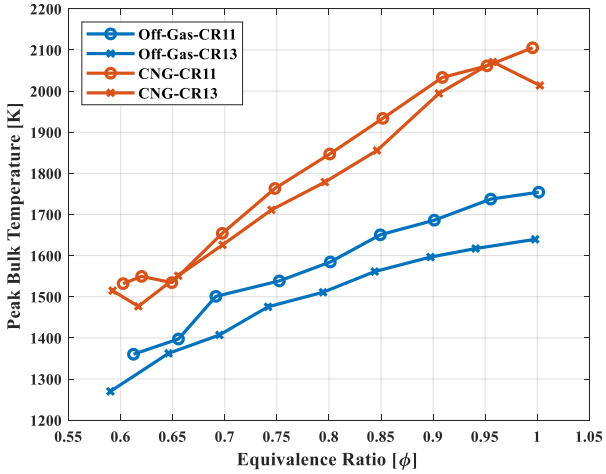

Figure 6. Peak cylinder temperature as a function of φ for the anode off-gas and CNG.

The emission index of NO_x with respect to ϕ, for the anode off-gas and CNG combustion, at CR of 11:1 and 13:1 is shown in Figure 7. It is well known that the formation of NO_x is dependent upon the peak cylinder temperature and oxygen availability in the mixture. As shown in the figure, as the charge ϕ is decreased from stoichiometry, the NO_x emissions are also decreased as a result of reduction in the peak cylinder temperature. Combustion with the anode off-gas resulted in negligible NO_x emissions compared to CNG, since the peak temperatures never exceeded 1800 K. Increasing the compression ratio from 11:1 to 13:1 resulted in slightly lower NO_x emissions, due to the lower cylinder temperatures caused by delayed combustion phasing.

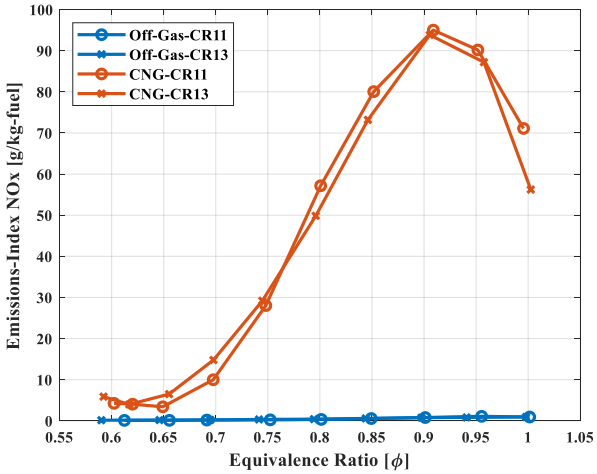

Figure 7. NO_x emissions as a function of φ for the anode off-gas and CNG.

The emission index of CO with respect to ϕ, for the anode off-gas and CNG combustion, at CR of 11:1 and 13:1 is shown in Figure 8. As the charge ϕ is decreased from stoichiometry to ϕ = 0.95, there is a notable decrease in engine-out CO emissions. As the charge ϕ is further decreased from ϕ = 0.95, there is a gradual increase in engine-out CO emissions. The reduction in CO is achieved when excess oxygen in a high temperature environment enables the reactants to form CO_2. As the target ϕ is reduced below stoichiometry, excess oxygen is available in the combustion chamber to react with CO. At the same time, as the charge-mixture ϕ is further decreased, the heat release is decreased, leading to lower overall cylinder temperatures. The optimum trade-off between increasing oxygen availability in the combustion chamber and cylinder temperatures remaining sufficiently high for CO to form CO_2 exists at ϕ = 0.95 for both the anode off-gas and CNG combustion. Increasing the compression ratio from 11:1 to 13:1 yielded a higher amount of engine-out CO attributed to the delayed combustion phasing and lower combustion efficiency (shown later). Combustion with CNG resulted in overall lower CO emissions compared to anode off-gas, due to the higher peak cylinder temperatures and the absence of CO in the unburned fuel-air mixture.

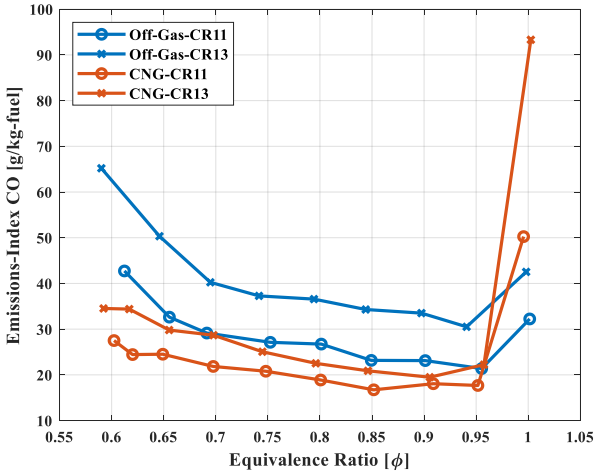

Figure 8. CO emissions as a function of φ for anode off-gas and CNG.

The combustion efficiency is a measure of how complete the combustion process is at converting reactants into products. For typical hydrocarbon fuels, the combustion efficiency is calculated based on the emissions of CO_2, THC, and CO. However, for the anode off-gas the combustion efficiency is more appropriately calculated based on only the CO content found in the exhaust. The following two formulas were used for the calculation of combustion efficiency for CNG and the anode off-gas:

$$\eta_{combustion} = 100 - \frac{100}{CO_2+CO+THC} * \left(\frac{254*CO+217.1*h_{2,dry}}{\dot{m}_{fuel}*LHV} + THC\right) \quad (3)$$

$$\eta_{combustion} = \frac{\dot{m}_{co,i}}{\dot{m}_{co,e}} \quad (4)$$

The THC emissions is expected to be negligible since there is no hydrocarbon species in the fuel mixture. The combustion efficiency with respect to ϕ, for the anode off-gas and CNG combustion, at CR

of 11:1 and 13:1 is shown in Figure 9. Overall, the combustion efficiency was reduced when the engine lean misfire limit was approached and when the mixture was close to stoichiometry. Between these two extremes, both fuels exhibited a plateau of combustion efficiency. The high combustion efficiency values in leaner conditions were favored by excess oxygen and sufficiently high cylinder temperatures. Increasing the compression ratio from 11:1 to 13:1 yields a lower combustion efficiency, which is due to the delayed combustion phasing and lower cylinder temperatures, which negatively affects the oxidation reactions. For the anode off-gas, the combustion efficiency is lower than CNG, since the peak cylinder temperature was reduced as a result of lower heat release rate and flame propagation speeds.

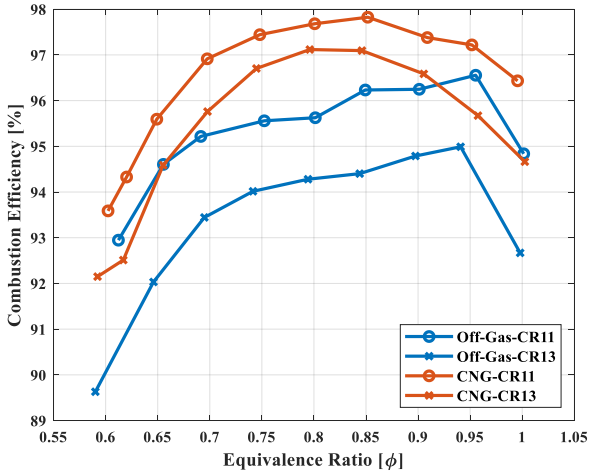

Figure 9. Engine combustion efficiency as a function of φ for anode off-gas and CNG.

The net indicated efficiency for combustion of anode off-gas and CNG with respect to ϕ at compression ratio of 11:1 and 13:1, is shown in Figure 10. Combustion with the anode off-gas resulted in net indicated efficiency of 31.2% at CR of 13:1, while combustion with CNG resulted in higher net indicated efficiency due to higher combustion efficiency and higher average ratio of specific heats (γ), as shown in Figure 11. The combustion phasing and burn duration was similar between the two fuels. As the equivalence ratio became progressively leaner, the net indicated efficiency increased due to higher γ and lower heat transfer loss. However, as the lean misfire limit is approached, the net indicated efficiency decreased due to the deterioration of combustion efficiency. Increasing the compression ratio resulted in marginally higher net indicated efficiency as a result of higher expansion ratio, partially offset by the delayed combustion phasing.

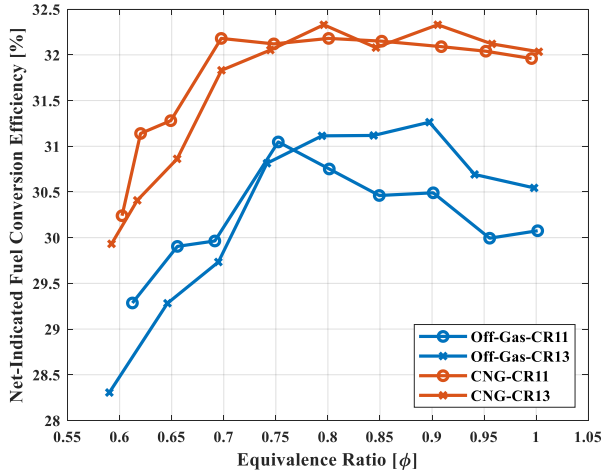

Figure 10. Net indicated efficiency as a function of φ for anode off-gas and CNG.

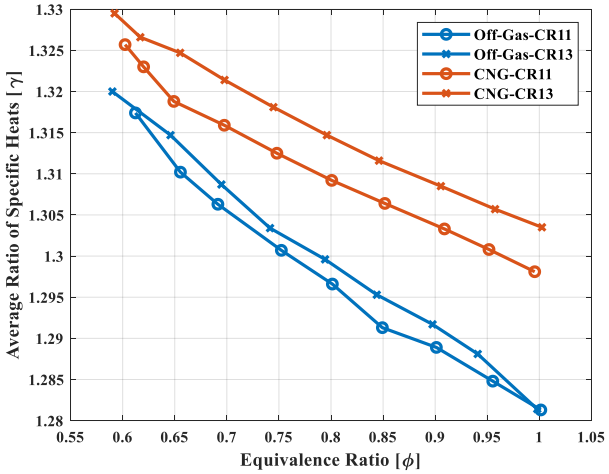

Figure 11. Average ratio of specific heats (γ) as a function of φ for anode off-gas and CNG.

The crank angle of 50% mass fraction burned (CA50) for the anode off-gas and CNG with respect to ϕ at compression ratio of 11:1 and 13:1, is shown in Figure 12. The CA50 values are used as a parameter to describe combustion phasing and were directly related to the spark timing. As shown in the figure, the CA50 at CR of 13:1 is phased later than that of 11:1, which is knock limited, particularly at higher equivalence ratios. As the mixture ϕ becomes leaner, the fuel input energy in the combustion chamber is less and thus the mixture is less susceptible to knocking. This allows the leaner air-fuel mixtures at CR of 13:1 to have similar CA50 timings as mixtures burned at CR of 11:1 to ensure optimal net indicated efficiency. The CA50 trend for both the anode off-gas and CNG demonstrated that combustion can be phased to achieve high fuel conversion efficiency and maintain stable combustion, which is attributed to their excellent anti-knock properties.

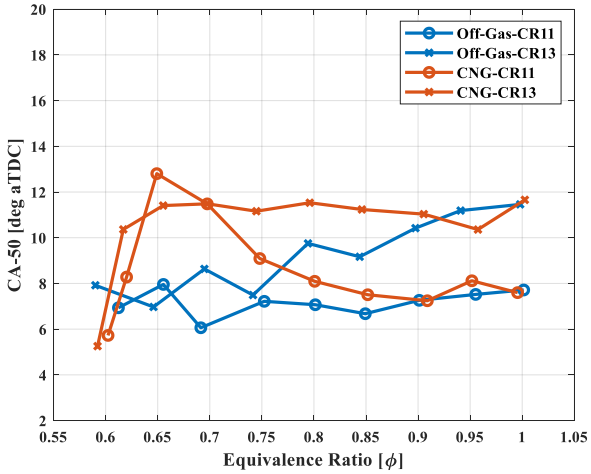

Figure 12. CA50 as a function of φ for anode off-gas and CNG

The fuel input energy distribution for the anode off-gas and CNG at compression ratio of 11:1 and stoichiometric operation is shown in Figure 13. Combustion with the anode off-gas resulted in significantly lower heat transfer loss than CNG, due to the greatly reduced cylinder temperatures. Both fuels showed similar gross work output, but the lower combustion efficiency with the off-gas negatively affects the net indicated efficiency. It is interesting to note that combustion with CNG results in higher cylinder temperatures as shown above, which increases the heat losses to the walls. However, the composition of the CNG-air mixture results in higher γ, which increases the thermal efficiency and thus the net indicated efficiency, as shown in Figure 9.

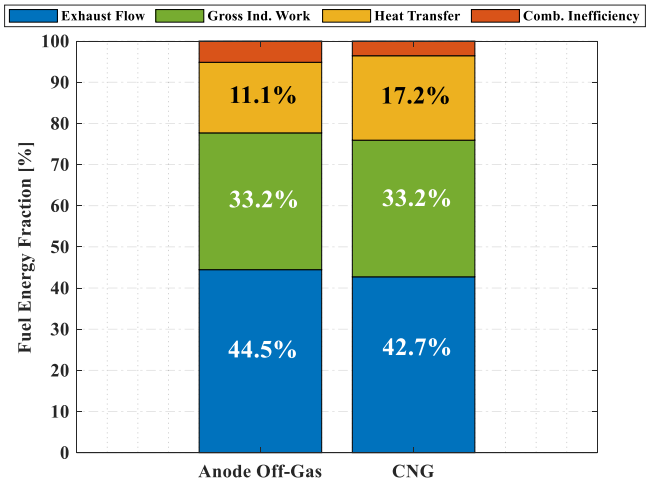

Figure 13. Fuel energy distribution for the anode off-gas and CNG.

Summary and Conclusions

A single-cylinder CFR engine was used in this experimental study to investigate spark ignition combustion with SOFC anode off-gas at two different compression ratios. The results were compared to combustion with CNG at the same engine operating conditions. The effect of the anode off-gas fuel properties and compression ratio on the combustion characteristics, emissions formation, and efficiency were quantified and analyzed. The key findings and conclusions can be summarized in the following:

- The composition of the anode off-gas is conducive to spark ignition combustion due to its H_2 and CO content. However, the anode off-gas also contains CO_2 and H_2O which act as diluents and reduce the volumetric efficiency of the engine.
- A single-cylinder CFR engine can successfully use the SOFC anode off-gas as a fuel in spark-ignition combustion mode to achieve 31.2% net indicated efficiency at compression ratio of 13:1.
- The anode off-gas can be used as a potential alternative fuel in spark-ignition engines to provide additional power in a SOFC-ICE hybrid system.
- Spark-ignition combustion with anode off-gas resulted in lower engine load than CNG at the same engine operating conditions due to lower energy content in the fuel, lower stoichiometric air-fuel ratio, and the presence of diluents that limit the heat release and the pressure rise.
- The NO_x emissions from anode off-gas combustion were negligible due to the low peak cylinder temperatures enabled by the diluents.
- The unburned hydrocarbon emissions were zero due to the absence of any hydrocarbon species in the anode off-gas.

Future work of the authors will utilize a modern spark-ignition engine platform, which is expected to yield higher fuel conversion efficiency from combustion with the anode off-gas.

References

1. Longwell, John P., Edward S. Rubin, and J. Wilson. "Coal: Energy for the future." *Progress in Energy and Combustion Science 21*, no. 4 (1995): 269-360.
2. Bizon, Nicu, and Phatiphat Thounthong. "Fuel economy using the global optimization of the Fuel Cell Hybrid Power Systems." *Energy conversion and management* 173 (2018): 665-678.
3. Sulaiman, N., M. A. Hannan, Azah Mohamed, Pin Jern Ker, E. H. Majlan, and WR Wan Daud. "Optimization of energy management system for fuel-cell hybrid electric vehicles: Issues and recommendations." *Applied energy 228* (2018): 2061-2079.
4. Song, Ke, Huan Chen, Peimin Wen, Tao Zhang, Boqiang Zhang, and Tong Zhang. "A comprehensive evaluation framework to evaluate energy management strategies of fuel cell electric vehicles." *Electrochimica Acta* 292 (2018): 960-973.
5. Lee, Young Duk, Kook Young Ahn, Tatiana Morosuk, and George Tsatsaronis. "Environmental impact assessment of a solid-oxide fuel-cell-based combined-heat-and-power-generation system." *Energy* 79 (2015): 455-466.
6. Brouwer, J., 2006. Hybrid gas turbine fuel cell systems, Chapter 4. The Gas Turbine Handbook, US Department of Energy, Morgantown, West Virginia.
7. Cheddie, Denver F. "Thermo-economic optimization of an indirectly coupled solid oxide fuel cell/gas turbine hybrid power plant." *International Journal of Hydrogen Energy* 36, no. 2 (2011): 1702-1709.
8. Inui, Y., T. Matsumae, H. Koga, and K. Nishiura. "High performance SOFC/GT combined power generation system with CO2 recovery by oxygen combustion method." *Energy Conversion and Management* 46, no. 11-12 (2005): 1837-1847.
9. Harvey, S. P., and H. J. Richter. "Gas Turbine Cycles With Solid Oxide Fuel Cells—Part I: Improved Gas Turbine Power Plant Efficiency by Use of Recycled Exhaust Gases and Fuel Cell Technology." *Journal of energy resources technology* 116, no. 4 (1994): 305-311.
10. Chan, S. H., H. K. Ho, and Y. Tian. "Multi-level modeling of SOFC–gas turbine hybrid system." *International Journal of Hydrogen Energy* 28, no. 8 (2003): 889-900.
11. Kuchonthara, Prapan, Sankar Bhattacharya, and Atsushi Tsutsumi. "Combinations of solid oxide fuel cell and several enhanced gas turbine cycles." *Journal of Power Sources* 124, no. 1 (2003): 65-75.
12. Calise, F., A. Palombo, and L. Vanoli. "Design and partial load exergy analysis of hybrid SOFC–GT power plant." *Journal of power sources* 158, no. 1 (2006): 225-244.
13. Vora, Shailesh D. "Office of Fossil Energy's Solid Oxide Fuel Cell Program Overview." In *15th Annual SECA Workshop, July*, pp. 22-23. 2014.
14. Owens, Brandon. "The rise of distributed power." *General Electric* 47 (2014).
15. Kim, J., Kim, Y., Choi, W., Ahn, K.Y. and Song, H.H., 2020. Analysis on the operating performance of 5-kW class solid oxide fuel cell-internal combustion engine hybrid system using spark-assisted ignition. *Applied Energy*, *260*, p.114231.
16. Fyffe, John R., Mark A. Donohue, Maria C. Regalbuto, and Chris F. Edwards. "Mixed combustion–electrochemical energy conversion for high-efficiency, transportation-scale engines." *International Journal of Engine Research* 18, no. 7 (2017): 701-716.
17. Choi, Wonjae, Jaehyun Kim, Yongtae Kim, Seonyeob Kim, Sechul Oh, and Han Ho Song. "Experimental study of homogeneous charge compression ignition engine operation fuelled by emulated solid oxide fuel cell anode off-gas." *Applied energy* 229 (2018): 42-62.
18. Ran, Zhongnan, Deivanayagam Hariharan, Benjamin Lawler, and Sotirios Mamalis. "Experimental study of lean spark ignition combustion using gasoline, ethanol, natural gas, and syngas." *Fuel* 235 (2019): 530-537.
19. Karim, Ghazi A. "Hydrogen as a spark ignition engine fuel." *International Journal of Hydrogen Energy* 28, no. 5 (2003): 569-577.
20. Korakianitis, T., A. M. Namasivayam, and R. J. Crookes. "Natural-gas fueled spark-ignition (SI) and compression-ignition (CI) engine performance and emissions." *Progress in energy and combustion science* 37, no. 1 (2011): 89-112.
21. Bach, Christian, Christian Lämmle, Rolf Bill, Patrik Soltic, David Dyntar, Philippe Janner, Konstantinos Boulouchos et al. *Clean engine vehicle a natural gas driven Euro-4/SULEV with 30% reduced CO2-emissions*. No. 2004-01-0645. SAE Technical paper, 2004.
22. Raman, P., and N. K. Ram. "Performance analysis of an internal combustion engine operated on producer gas, in comparison with the performance of the natural gas and diesel engines." *Energy* 63 (2013): 317-333.
23. Mustafi, N. N., Y. C. Miraglia, R. R. Raine, P. K. Bansal, and S. T. Elder. "Spark-ignition engine performance with 'Powergas' fuel (mixture of CO/H2): A comparison with gasoline and natural gas." *Fuel* 85, no. 12-13 (2006): 1605-1612.
24. Heywood, John B. "Internal combustion engine fundamentals." (1988).

Contact Information

Corresponding author:

Zhongnan Ran
zhongnan.ran@stonybrook.edu
Department of Mechanical Engineering
Stony Brook University
Stony Brook, NY, 11794, USA

Acknowledgments

This research study was supported by the U.S. Department of Energy ARPA-E INTEGRATE program, under award number DE-AR0000959 to Stony Brook University. The authors would like to thank Mr. Gene Arkenberg and Dr. Scott Swartz from Nexceris, LLC for providing information regarding the anode off-gas composition and overall SOFC operating characteristics.

Definitions/Abbreviations

CAD – Crank Angle Degree

CNG – Compressed Natural Gas

COV – Coefficient of Variance

CR – Compression Ratio

GT – Gas Turbine

ICE – Internal Combustion Engine

***IMEP$_{net}$* –** Net Indicated Mean Effective Pressure

LHV – Lower Heating Value

MBT – Maximum Brake Torque

RON – Research Octane Number

SI – Spark-Ignition

SOFC – Solid Oxide Fuel Cell

THC – Total Hydrocarbon